Available online at www.sciencedirect.com
SCIENCE DIRECT®
Journal of Nuclear Materials 348 (2006) 122–132
journal of nuclear materials
www.elsevier.com/locate/jnucmat

Thermal, structural, and radiological properties of irradiated graphite from the ASTRA research reactor – Implications for disposal

Dusan Lexa [a,*], A. Jeremy Kropf [b]

[a] Department of Radioactive Waste Management, Nuclear Engineering Seibersdorf GmbH, 2444 Seibersdorf, Austria
[b] Chemical Technology Division, Argonne National Laboratory, Argonne, IL 60439, USA

Received 26 July 2005; accepted 14 September 2005

Abstract

The release of Wigner energy from the graphite of the inner thermal column of the ASTRA research reactor has been studied by differential scanning calorimetry and simultaneous differential scanning calorimetry/synchrotron powder X-ray diffraction between 25 °C and 725 °C at a heating rate of 10 °C min^{-1}. The graphite, having been subject to a fast-neutron fluence from $\sim 10^{17}$ to $\sim 10^{20}$ n cm^{-2} over the life time of the reactor at temperatures not exceeding 100 °C, exhibits Wigner energies ranging from 25 to 572 J g^{-1} and a Wigner energy accumulation rate of $\sim 7 \times 10^{-17}$ J g^{-1}/n cm^{-2}. The shape of the rate-of-heat-release curves, e.g., maximum at ca. 200 °C and a fine structure at higher temperatures, varies with sample position within the inner thermal column, i.e., the distance from the reactor core. Crystal structure of samples closest to the reactor core (fast-neutron fluence $>1.5-5.0 \times 10^{19}$ n cm^{-2}) is destroyed while that of samples farther from the reactor core (fast-neutron fluence $<1.5-5.0 \times 10^{19}$ n cm^{-2}) is intact, with marked swelling along the *c*-axis. The dependence of the *c* lattice parameter on temperature between 25 °C and 200 °C as determined by Rietveld refinement for the non-amorphous samples leads to the expected microscopic thermal expansion coefficient along the *c*-axis of $\sim 26 \times 10^{-6}$ °C^{-1}. However, at 200 °C, coinciding with the maximum in the rate-of-heat-release curves, the rate of thermal expansion abruptly decreases indicating a crystal lattice relaxation. The ^{14}C activity in the inner thermal column graphite ranges from 6 to 467 kBq g^{-1}. The graphite of the inner thermal column of the ASTRA research reactor has been treated by heating to 400 °C for 24 h in a hot-cell facility prior to interim storage.

PACS: 81.05.T; 61.80; 81.70.P; 61.60

1. Introduction

Displacement of atoms from their normal lattice positions in solids by fast particles was first predicted by Wigner in 1942 [1]. The resulting entrapment of these atoms at non-lattice points is accompanied by a number of changes in physical

* Corresponding author. Tel.: +43 50550 2601; fax: +43 50550 2603.
E-mail address: dusan.lexa@arcs.ac.at (D. Lexa).

0022-3115/$ - see front matter © 2005 Elsevier B.V. All rights reserved.
doi:10.1016/j.jnucmat.2005.09.010

characteristics of the solid, including an increase in internal energy, also called Wigner energy. These effects have most frequently been observed and studied in graphite irradiated by fast neutrons [2], and are especially pronounced following graphite irradiation at low temperatures, i.e., below 100 °C, where no significant in situ annealing takes place – conditions also encountered in research reactors. Uncontrolled release of Wigner energy can, under certain circumstances, lead to the oxidation of graphite, as was the case with the Windscale Pile 1 reactor in 1957. Hence, the Wigner energy content of any irradiated graphite slated for disposal should be assessed and taken into account in selecting and implementing an appropriate treatment and disposal option. The presence of significant quantities of ^{14}C in irradiated graphite presents additional difficulties in this respect. These and other problems in nuclear graphite waste management have been recounted elsewhere [3].

The ASTRA reactor (Fig. 1) – a 10 MW light water moderated and cooled pool type research reactor in operation in Seibersdorf, Austria, between 1960 and 1999 – is undergoing decommissioning [4]. The bulk of the resulting material exhibits activities below applicable clearance levels, e.g., the concrete blocks cut from the biological shield, with the exception of activated core- and close-to-core structures as well as some radioactively contaminated components. The activated and/or contaminated material is being treated, conditioned, and stored on site. This applies, inter alia, to approximately 10 tons of reactor-grade graphite from the inner and outer thermal columns of the

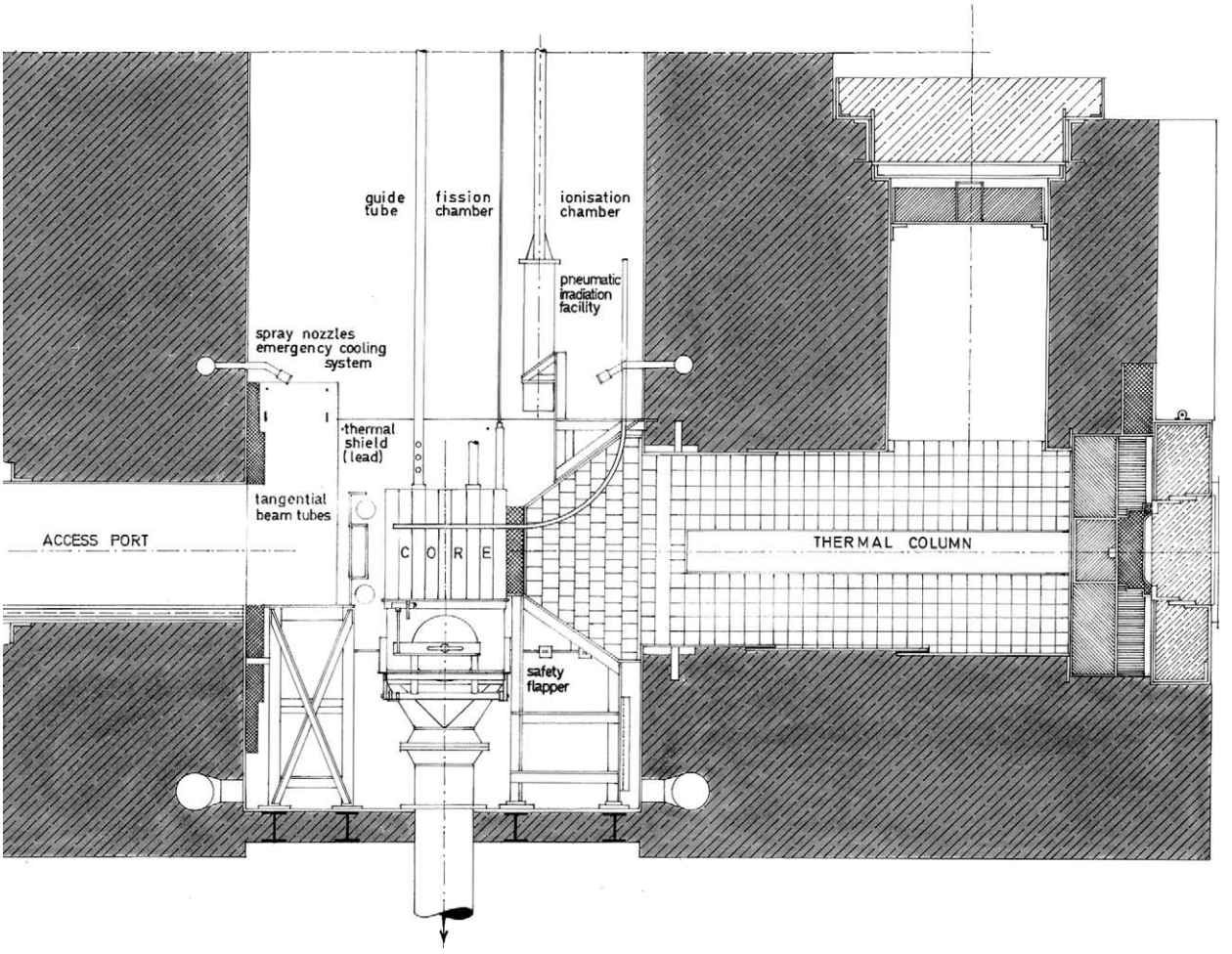

Fig. 1. Vertical section of the ASTRA research reactor block. Pyramidal inner thermal column and a rectangular outer thermal column with the 10 cm × 10 cm faces of the graphite blocks clearly visible.

reactor in the form of blocks 10 cm × 10 cm × (60–100) cm. Over the 40 years of reactor operation, the graphite has been exposed to significant fast-neutron fluence, roughly estimated at up to 10^{20} n cm^{-2} at temperatures not exceeding 100 °C. Preliminary measurements also suggested that the activity of the main slow-neutron activation product, ^{14}C, in the graphite from the outer thermal column was on the order of 1 kBq g^{-1}, with other radionuclides, e.g., ^{60}Co and ^{152}Eu, present in trace amounts. Larger activities were expected in the inner thermal column graphite.

To support the treatment, conditioning, interim storage, and final disposal of this material, it was necessary to quantify the Wigner energy content of the material and to understand the release of Wigner energy in the course of a relatively fast heat-up to a high temperature, emulating the thermal treatment of the material. (It became clear after the first heat-up experiments with individual blocks in a hot-cell facility that significant amounts of Wigner energy were indeed being released since the temperature indicated by a thermocouple embedded in the block was higher than the furnace control thermocouple during the first heat-up but lagged behind it during the second one. Hence, storage of the material without thermal treatment was deemed unacceptable.) In addition to addressing these practical concerns, there was the possibility of gaining deeper insight into the Wigner energy phenomenon per se. This was due, in particular, to the availability of estimated fast-neutron fluence data for any position within the graphite thermal columns. Because of the gradual decay of the fluence with distance from the reactor core, samples of graphite spanning a wide range of fluences were available. Hence, the amount of Wigner energy stored and released and associated crystal structure changes in the graphite could be studied as a function of fluence.

2. Experimental

The pyramidal inner thermal column (Fig. 1), with the maximum expected accumulation of Wigner energy, has been sampled by core drilling at seven positions along the column's longitudinal axis labeled a–g, with distances from the surface near the reactor core ranging from 0.0 (g) to ~0.6 (a) m. (The outer thermal column has not been sampled.) Five samples from each position were machined: three simple disks, 8.0 mm in diameter and 1.0 mm thick, weighing ~80 mg, for differential scanning calorimetry (DSC), and two two-layer-wedding-cake disks, with an 8.0 × 0.5 mm base and a 6.0 × 0.5 mm top, weighing ~65 mg, one for DSC and one for simultaneous differential scanning calorimetry/synchrotron powder X-ray diffraction (DSC/XRD). Machining of the samples on a lathe was done at reduced rpm with alcohol cooling so that the temperature is not expected to have exceeded 25 °C. The graphite specifications are summarized in Table 1.

DSC experiments were performed with power-compensated instruments Perkin–Elmer DSC-7 and Perkin–Elmer Pyris Diamond. The DSC-7 settings were: ice-water cooling (0 °C), 99.9999%

Table 1
Graphite specifications[a]

Type	Artificial graphite baked at not less than 4500 °F
Thermal neutron cross section	4.8 mb/atom
Average diffusion length	not less than 48 cm
Total ash content	700 ppm
Boron	0.8 max ppm
Porosity	24–25%
Specific resistance (ohm in)	longitudinal: 0.00030/transverse: 0.00040
Tensile strength (psi)	1400
Flexural strength (psi)	2100
Compressive strength (psi)	6000
Modulus of elasticity × 10^6 (psi)	longitudinal: 1.5/transverse: 1.1
Thermal conductivity (Btu/h/ft^2/°F/ft)	longitudinal: 90–100/transverse: 65–75
Coefficient of thermal expansion × 10^{-7}/°F	longitudinal: 8/transverse: 15
Apparent density (g/cm^3)	1.68–1.70

[a] The graphite has originally been manufactured by the American Machine & Foundry Company in 1958. These specifications are a verbatim transcription, including the original units, of a data sheet provided by the manufacturer at that time.

Ar purge gas at 20 $cm^3\,min^{-1}$, temperature range 25–625 °C, heating rate 10 °C min^{-1}, and sample weight ~65 mg. The Pyris Diamond settings were: circulating-liquid chiller cooling (−5 °C), 99.9999% Ar purge gas at 20 $cm^3\,min^{-1}$, temperature range 25–725 °C, heating rate 10 °C min^{-1}, and sample weight ~80 mg.

DSC/XRD experiments were performed on the Sector 10 insertion device beam line (Materials Research Collaborative Access Team) at the Advanced Photon Source, Argonne National Laboratory, with an instrument described previously [5]. It essentially consists of a Perkin–Elmer DSC sample holder modified to allow for simultaneous XRD, attached to a diffractometer, and a remotely connected Perkin–Elmer Pyris 1 DSC instrument. The Pyris 1 DSC settings were: circulating-liquid chiller cooling (−10 °C), 99.9999% Ar purge gas at 20 $cm^3\,min^{-1}$, temperature range 25–525 °C, heating rate 10 °C min^{-1}, and sample weight ~65 mg. Each DSC scan was accompanied by a full 2θ XRD scan every 10 °C. A cryogenically-cooled Si(1 1 1) double-crystal monochromator was used to select the incident beam wavelength of 0.082650 nm (15.000 keV). Higher energy harmonics were rejected by a polished, uncoated, ULE glass mirror. The resolution of the instrument was set by the convolution of the incident beam size (0.35 mm × 0.50 mm $V \times H$) with the acceptance of the double slit collimator in front of the detector (0.65 mm × 2.5 mm, 650 mm from the sample). The resulting 2θ resolution was about 0.06° (FWHM). X-rays were detected by an Oxford–Danfysik NaI scintillation detector. The detector was scanned from 4° to 45° at a rate of 1° s^{-1}, with data points acquired in 0.015 s bins, for a data point spacing of 0.015°. The 2θ axis was scanned both up and down to minimize the lost time between scans. XRD patterns were evaluated by Rietveld refinement using the GSAS software package [6] with only background, profile coefficients, histogram scale factors, diffractometer zero, absorption correction, and lattice parameters c and a being optimized.

In both DSC and DSC/XRD experiments, two identical scans were performed with each sample. The heat flux measured by DSC in the first run is a result of the sample heat capacity and the release of the Wigner energy, while in the second run only heat capacity should contribute to the heat flux, assuming complete Wigner energy release in the first run. (This assumption has been checked by subjecting one of the e samples to a total of five consecutive scans. No appreciable difference could be observed between the last four scans. See also Section 3.) Hence, subtraction of the second-run from the first-run data (including, in some cases, a linear correction for baseline drift), division by sample mass, and integration over a specified temperature range, yields the specific Wigner energy released in the first run.

The ^{14}C analyses were performed by combustion of ~300 mg graphite powder that remained after machining the DSC and DSC/XRD sample disks at 800 °C in an O_2 atmosphere within a Carbolite® oven. The off-gases were bubbled through two impingers each filled with 40 ml 4 N NaOH solution in order to absorb the CO_2. One milliliter aliquots of these solutions were mixed with 15 ml Ultima Gold XR liquid scintillation cocktail and counted in a Wallac Quantulus liquid scintillation counter. In another aliquot of the solution, the CO_3^{2-} concentration was determined with an Eltra CS 500 carbon–sulphur analyser equipped with a TIC-module. CO_2 is liberated from the solution upon addition of excess 50% H_3PO_4, stripped with a stream of O_2, and the concentration determined with an IR detector. The recovery of C was determined to be 85–100%. The absorption of CO_2 was nearly quantitative in the first impinger, while the second one exhibited C concentrations two orders of magnitude lower. The incomplete recovery of C in some cases was attributed to the formation of CO which is not absorbed by NaOH.

3. Theory and calculations

Displacement of atoms from their normal lattice positions in solids by fast particles was first predicted by Wigner in 1942 [1]. He showed that fast neutrons produced in the fission of uranium would possess enough energy to displace $\sim 2 \times 10^4$ carbon atoms per neutron. Subsequent calculations by Seitz [7] put the number closer to $\sim 2 \times 10^3$. The resulting entrapment of the displaced atoms at non-lattice points and the creation of vacancies are accompanied by a number of changes in physical characteristics of the solid, such as a decrease in thermal conductivity and a lattice parameter, and an increase in elastic modulus, electrical resistance, breaking strength, c lattice parameter and internal (Wigner) energy [2].

Upon heating to sufficiently high temperatures, the displaced atoms presumably diffuse back to the vacancies. The energy, released as heat, can be measured by standard calorimetry techniques. The

magnitude of the Wigner energy in graphite has first been measured using a simple DTA apparatus [2]. Samples irradiated at the Oak Ridge graphite pile for 54 MW-days at <100 °C and 175 MW-days at <130 °C exhibited an energy release of 9 J g^{-1} and 29 J g^{-1}, respectively, upon heating from room temperature to 300 °C at 2 °C min^{-1}. Heating to 500 °C increased these values by an estimated 10%. Iwata [8] has investigated the magnitude and the kinetics of the Wigner energy release from graphite irradiated to a fluence of 4×10^{17} n cm^{-2} at ~80 °C by DTA between room temperature and 350 °C at heating rates from 1 to 100 °C min^{-1}. He obtained a value of 8 ± 1 J g^{-1} and proposed a kinetic model of the Wigner energy release involving three activation energies. Preston and Melvin [9] have measured samples from a Windscale Pile 2 dowel by DSC between 40 and 150 °C at heating rates between 0.1 and 30 °C min^{-1} with an isothermal hold at the upper temperature. The highest Wigner energy release observed was 135 J g^{-1}. (A single sample was heated to 600 °C at 10 °C min^{-1} with a Wigner energy release of 262 J g^{-1}.) Unfortunately, the dose history and location of the dowel in the Pile are unknown. Based on this and other studies on Wigner energy release from Windscale Pile 1 and 2 graphite, Minshall and Wickham [10] developed a kinetic model of the Wigner energy release involving a spectrum of activation energies which was used to assess the significance of the Wigner energy for the disposal of graphite [11]. Wörner et al. [12] have studied Wigner energy release from Windscale Pile 2 graphite by DSC between 50 and 400 °C at 25 °C min^{-1}. For a sample with an extrapolated Wigner energy release of 220 J g^{-1} between 50 and 500 °C, the fraction of energy released by heating to 300 °C is 0.90. (This also confirms the assumption of complete Wigner energy release in the first of the two DSC runs performed at a lower heating rate of 10 °C min^{-1} and to a higher temperature of between 525 and 725 °C, see Section 2.) Hence, treatment of the Windscale Pile graphite by heating to 300 °C for 30 min has been proposed by the authors as a sensible alternative to the previously suggested 400 °C which, in addition, would result in lower ^3H emissions. The effects of fluence and irradiation temperature on Wigner energy accumulation and release have been reviewed by Kelly et al. [13]. The Wigner energy content exhibits saturation at high fluences and there is a large effect of irradiation temperature, the rate of energy accumulation decreasing with increasing temperature.

The effective heat capacity of irradiated graphite, c'_p, is defined as

$$c'_p = c_p - \frac{dH}{dT}, \tag{1}$$

where c_p is the normal heat capacity of graphite and dH/dT is the heat release per unit temperature rise. If c'_p is negative over a temperature range, the material is self-heating and the possibility of a large temperature rise exists. For simplicity, the worst-case scenario of an adiabatic energy release at a constant heat capacity is considered here. The associated temperature rise is then given by

$$\Delta T_{max} = \frac{\Delta H_{Wigner}}{c_p}, \tag{2}$$

where the value of c_p be taken as 1 J $°C^{-1}$ g^{-1}. (c_p actually varies between 1 J $°C^{-1}$ g^{-1} at 100 °C and ~2 J $°C^{-1}$ g^{-1} at 1000 °C.) Reaching temperatures above ~400 °C is considered sufficient for thermal oxidation [13].

Kelly et al. [13] also reviewed the dimensional changes and the thermal expansion coefficient of irradiated graphite. Generally, expansion in the direction perpendicular to the basal planes (c) and contraction in the direction parallel to them (a) has been observed, although the relative magnitudes of the changes depend upon the exposure conditions. X-ray diffraction patterns of highly irradiated graphite exhibit broad and asymmetric peaks suggesting a decrease in the degree of crystallinity. The lattice parameter changes seem to be linear with fluence up to a fluence of 3×10^{18} n cm^{-2}. An experiment at 150 °C yielded a 13% increase in $\Delta c/c$ at a fluence of 1.6×10^{21} n cm^{-2} with a continued increase at a reducing rate.

There is still mostly speculation about the nature of the Wigner energy buildup and release at the atomic level. The recombination of interstitials and vacancies, also known as Frenkel pairs, is considered to be the key step in Wigner energy release. The energy of a widely spaced Frenkel pair has been reviewed by Thrower and Mayer [14] and given as 14 ± 1 eV. In their quantum-mechanical study, Telling et al. [15] concluded that a number of defect species form strong covalent bonds between the graphite atomic layers, calculated the energy released in a Frenkel pair recombination as 13–15 eV per pair, and also introduced a close-bound or intimate Frenkel pair with an energy of formation of 10.6 eV and a barrier to recombination of 1.4 eV. In another quantum-mechanical study,

Ewels et al. [16] examined the structures and recombination routes for Frenkel pairs in irradiated graphite. The energy of formation of a widely separated Frenkel pair is calculated as 13.7 eV, while that of the intimate Frenkel pair is given as 10.8 eV with and a barrier to recombination of 1.3 eV. The recombination of the intimate Frenkel pair is suggested as the cause of the Wigner energy release peak observed around 200 °C.

The connection between the fast-neutron fluence, Φ_f, and the number of atoms displaced, i.e., the number of Frenkel defects formed, is provided by the displacement cross section, σ_d:

$$n_F = \sigma_d \cdot \Phi_f \tag{3}$$

with n_F equivalent to the displacements per atom (dpa) if dpa < 1. The displacement cross section of graphite (and other materials) has been the subject of intense study. The results have been summarized by Iwata et al. [17]. The value for graphite, also used in [8], is 11.5×10^{-22} cm^2. Hence, using Eq. (3), the dpa can be calculated for any sample a–g provided the value of Φ_f at sample location is known. At the same time, a simple relationship between Wigner energy, ΔH_{Wigner} (J g^{-1}), Frenkel defect energy, h_F (eV), and n_F can be established:

$$n_F = \frac{M_C}{N_A} \frac{\Delta H_{Wigner}}{1.602 \times 10^{-19} h_F}, \tag{4}$$

where N_A is Avogadro's number, and M_C is the molar mass of graphite. This equation enables the dpa calculation from the experimentally determined ΔH_{Wigner} and the theoretical value of h_F. Ideally, the dpa values obtained from Eqs. (3) and (4) should be identical. Any discrepancies would point to inaccuracies in one or more of the values of ΔH_{Wigner} (directly measured), Φ_f (indirectly measured), σ_d (indirectly measured), and h_F (theoretical).

In order to be able to correlate the thermal and structural data obtained in the course of this work with fast-neutron fluence, its profile within the inner thermal column was needed. The original idea was to reconstruct the fluence profile from the available reactor operation records. However, having the calculations performed turned out to be a major effort associated with very high cost (~$300 000). As a result, the fluence was estimated from all available information, including previous measurements at various irradiation positions, reactor core and thermal column geometry, and the known attenuation characteristics of water (pool), lead (shield), aluminum (liner), and graphite for fast neutrons (see Fig. 1) [18]. The dependence of the fast-neutron fluence ($E > 0.1$ MeV), Φ_f, on distance from the reactor core center, d, within the inner thermal column takes on the form:

$$\Phi_f(d) = \Phi_{f,0} \frac{d_0^2}{d^2} \exp\left(-\frac{d - d_0}{\lambda_r}\right) \tag{5}$$

with the fluence at the front face of the thermal column, at a distance of $d_0 = 52.2$ cm from the reactor core center, of $\Phi_{f,0} = 1.7 \times 10^{20}$ n cm^{-2}, and the relaxation length of graphite of $\lambda_r = 11$ cm. Hence, the fluence spans the range from $\Phi_{f,0}$ down to $\Phi_f = 6.4 \times 10^{16}$ n cm^{-2} at the rear face of the thermal column ($d = 120.6$ cm).

Even though scattering of fast neutrons is responsible for the Wigner energy buildup in graphite, the activity of ^{14}C – the main thermal neutron activation product in graphite – has also been measured. ^{14}C is produced from ^{13}C (1.11%) by the ^{13}C(n,γ)^{14}C reaction and from ^{14}N by the ^{14}N(n,p)^{14}C reaction with cross sections of $\sigma = 0.9 \pm 0.2$ mb and $\sigma = 1.81 \pm 0.05$ b, respectively [19]. ^{14}C does not undergo further activation to any significant extent and, with a half life of 5736 years, it is an excellent measure of the thermal neutron fluence which can be inferred from measured ^{14}C activities using an analog of Eq. (3). In addition, the presence of significant quantities of ^{14}C in irradiated graphite is another major factor in selecting and implementing any disposal option.

4. Results and discussion

A set of DSC plots obtained with one set of samples a–g in the course of a DSC/XRD experiment is shown in Fig. 2. Samples a–e exhibit a maximum rate of heat release around 200 °C and a negligible heat release at 525 °C. The character of the DSC plot obtained with samples f and g is entirely different in that no sharp peak at 200 °C is present and significant heat release continues at 525 °C. The disappearance of the 200 °C peak in highly irradiated graphite has been noted previously [13]. The graphite c_p curve indicates that for samples c–e, and g, the effective heat capacity, c_p', as defined by Eq. (1) is negative over an increasing temperature range beginning at ~175 °C with the associated potential for self-heating. Interestingly, even though sample f exhibits the second largest Wigner energy release, its rate-of-heat-release curve is such that c_p' is positive throughout the temperature range. In addition,

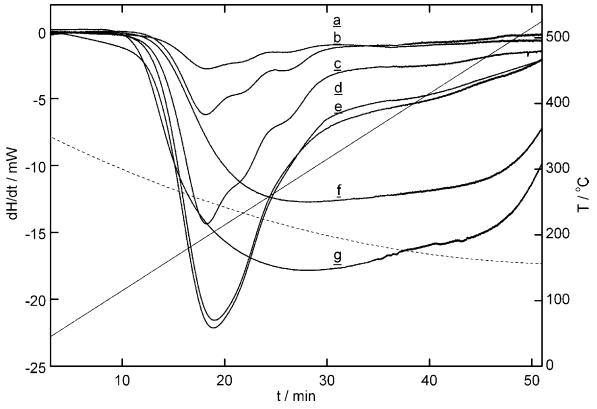

Fig. 2. DSC curves obtained between 25 °C and 525 °C at 10 °C min^{-1}. Sample mass ~65 mg, heavy line – heat flow, thin line–temperature, dashed line – heat flow due to c_p of graphite.

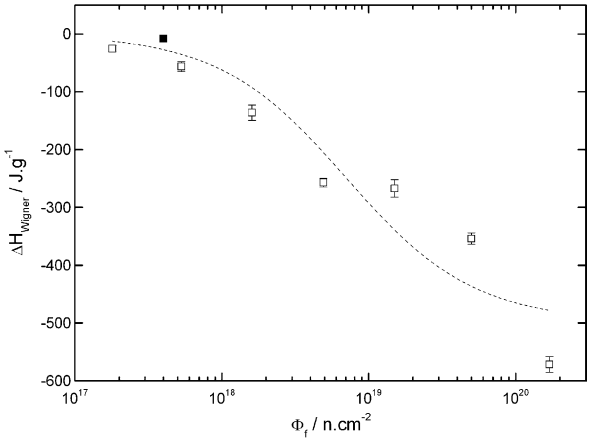

Fig. 3. ΔH_{Wigner} released between 25 °C and 525 °C at 10 °C min^{-1} as a function of fast-neutron fluence: (□) experimental data, (■) Iwata [8].

samples a–c show two additional peaks at higher temperatures initially described by Iwata [8]. This so called fine structure is apparently a signature of processes with higher activation energy than the Frenkel pair recombination responsible for the 200 °C peak. The elucidation of these processes would, however, require a separate study.

Integration of the DSC plots between 25 °C and 525 °C yields directly the Wigner energy released within this temperature range. Even though some of the data extend to 625 or 725 °C, the upper integration limit was kept at 525 °C for consistency. Furthermore, the Wigner energy release above 525 °C at 10 °C min^{-1} proved to be insignificant. The results are given in Table 2 as well as in Fig. 3. Each data point is an average of measurements on five samples. The Wigner energy ranges from 25 J g^{-1} for sample a to 572 J g^{-1} for sample g. The dependence of Wigner energy on fluence could reasonably be expected to be linear at low fluence values and exhibit saturation at high values. Hence, a simple empirical rational function was used to perform a least-squares fit to the data:

$$\Delta H_{\text{Wigner}}(\Phi_{\text{f}}) = \frac{a \cdot \Phi_{\text{f}}}{b + \Phi_{\text{f}}}. \tag{6}$$

The saturation value is $a = 500 \pm 66$ J g^{-1}, and the value of fluence that leads to a Wigner energy accumulation of one half the saturation value is $b = 7 \times 10^{18}$ n cm^{-2}. The slope of the ΔH_{Wigner} vs. Φ_{f} curve at zero fluence (Wigner energy accumulation per unit of fluence in the linear region) is $a/b = 7 \times 10^{-17}$ J g^{-1}/n cm^{-2}. This compares with the value of 2×10^{-17} J g^{-1}/n cm^{-2} derived from Iwata's data [8] (8 J g^{-1}/4×10^{17} n cm^{-2}). The fluence at which the Wigner energy accumulation begins to significantly deviate from linearity (e.g., $\Delta H_{\text{Wigner}} \leqslant 0.9a/b\Phi_{\text{f}}$) is $1/9b \approx 8 \times 10^{17}$ n cm^{-2}. This agrees rather well with the value of 10^{18} n cm^{-2} given in [14]. The adiabatic temperature rise according to Eq. (2) is also given in Table 2. Samples g and

Table 2
Sample characteristics, measured and derived quantities

Sample	d (cm)	Φ_{f} (n cm^{-2}) (Eq. (5))	dpa (Eq. (3))	ΔH_{Wigner} (J g^{-1})	dpa (Eq. (4))	$\Delta T_{\max}$ (°C) (Eq. (2))	c at 25 °C (nm)	$a_{\text{C-14}}$ (kBq g^{-1})
g	52.2	1.7×10^{20}	2.0×10^{-1}	-572 ± 14	5.1×10^{-3}	570	0.778[a]	467 ± 47
f	62.0	5.0×10^{19}	5.8×10^{-2}	-354 ± 10	3.1×10^{-3}	350	0.778[a]	64 ± 6
e	71.7	1.5×10^{19}	1.7×10^{-2}	-267 ± 15	2.4×10^{-3}	270	0.684	26 ± 3
d	81.5	4.9×10^{18}	5.6×10^{-3}	-257 ± 7	2.3×10^{-3}	260	0.683	37 ± 4
c	91.3	1.6×10^{18}	1.8×10^{-3}	-136 ± 13	1.2×10^{-3}	140	0.676	17 ± 2
b	101.1	5.3×10^{17}	6.1×10^{-4}	-56 ± 9	5.0×10^{-4}	60	0.675	14 ± 1
a	110.8	1.8×10^{17}	2.1×10^{-4}	-25 ± 5	2.2×10^{-4}	30	0.675	6 ± 1

[a] Calculated from the Bragg equation $\lambda = 2(c/2) \cdot \sin\theta$ for $2\theta = 12.2°$ and $\lambda = 0.082650$ nm.

possibly f could conceivably undergo thermal oxidation. However, only sample g has been shown to be self-heating over a wide temperature range. Thus it is the only sample presenting a real hazard in this respect. These considerations suggest that, prior to interim storage or final disposal, thermal treatment of the ASTRA graphite as well as graphite irradiated under similar conditions to a fast-neutron fluence higher than $\sim 5 \times 10^{19}$ n cm^{-2} should be considered. It is interesting to note that the Wigner energy release exhibited by sample d is significantly higher than a simple interpolation between c and e would suggest. This would imply a fast-neutron fluence peak in the middle of the inner thermal column – a rather unusual proposition.

A low-angle section of a set of XRD patterns taken at 25 °C at the beginning of the DSC/XRD scans is shown in Fig. 4. The 0 0 2 graphite diffraction peak at ~14° is very sharp in samples a–e and its position is such that the c lattice parameter increases in the same order. The 0 0 2 peak is missing in samples f and g, being replaced by a single broad peak at ~12.2° ($c = 0.778$ nm). This correlates well with the different DSC plot character in samples f and g. Hence, a fast-neutron fluence of somewhere between 1.5×10^{19} n cm^{-2} (e) and 5×10^{19} n cm^{-2} (f) was sufficient to render the original graphite crystal structure amorphous. The amorphous character of a sample increases with the number of atoms displaced from their normal lattice positions (dpa). A rough estimate from Fig. 5 puts the dpa of samples f and g at 0.1. The dpa values for all samples calculated from Eqs. (3) and (4) (with $h_F = 14$ eV [14]) are given in Table 2. The agreement for samples a–c is surprisingly good but deteriorates progressively for samples d–g. Considering the character of the quantities involved in Eqs. (3) and (4) (see Section 3), it seems most likely that the simple model presented by Eq. (4) breaks down at higher fast-neutron fluence values, i.e., h_F is no longer constant and independent of dpa. In fact there are indications that the h_F decreases substantially for dpa > 0.1 [13]. This would explain the observed underestimation of dpa at higher fluence values by Eq. (4). Taking the dpa from Eq. (3) and substituting back to Eq. (4) yields h_F values of between 5.7 eV (d) and 0.4 eV (g).

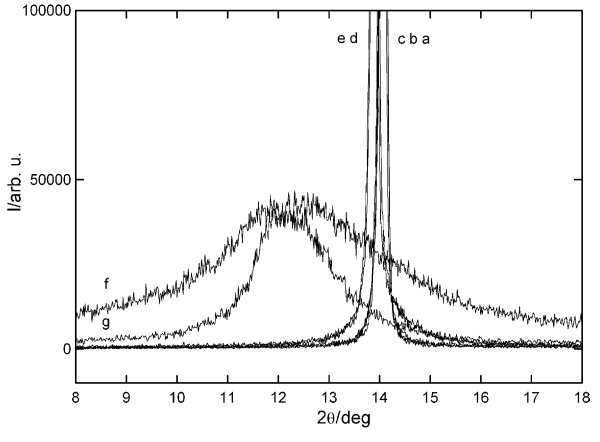

Fig. 4. Section of X-ray diffraction patterns at 25 °C in the vicinity of the 0 0 2 graphite diffraction peak.

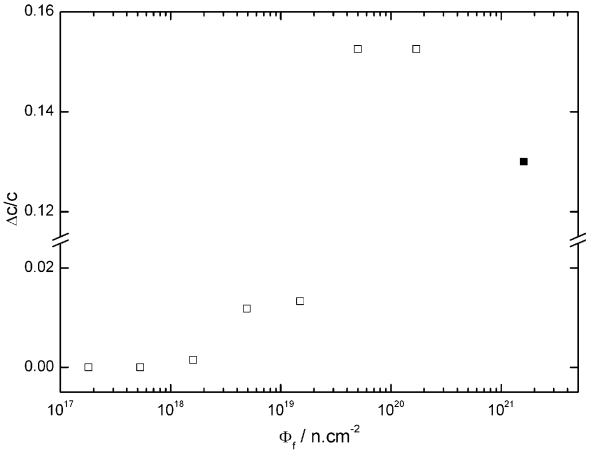

Fig. 5. Graphite c lattice parameter from Rietveld refinement with X-ray diffraction patterns obtained at 25 °C as a function of fast-neutron fluence: (□) experimental data, (■) Kelly et al. [13]. (Values for f and g calculated from the Bragg equation $\lambda = 2(c/2) \cdot \sin\theta$ for $2\theta = 12.2°$ and $\lambda = 0.082650$ nm.)

The graphite c lattice parameter obtained from Rietveld refinement using the XRD patterns taken at 25 °C is given in Table 2. In Fig. 5, $\Delta c/c$ is plotted as a function of fluence. Marked swelling along the c-axis is seen at 25 °C (for unirradiated graphite, $c = 0.672$ nm). The dependence of $\Delta c/c$ on on fluence is sigmoid with an inflection point between c and d. Hence, the nature of the defects leading to the increase in the c lattice parameter changes at a fluence of $1.6–4.9 \times 10^{18}$ n cm^{-2}. Incidentally, this is also where the DSC fine structure disappears. For comparison, a literature value [13] is also included in Fig. 5. The changes in the graphite c lattice parameter obtained as a result of Rietveld refinement using the XRD patterns from samples a–e between 25 °C and 525 °C are shown in Fig. 6. (The graphite a lattice parameter did not exhibit any measurable changes.) Between 25 °C and 180–190 °C, the samples undergo thermal expansion

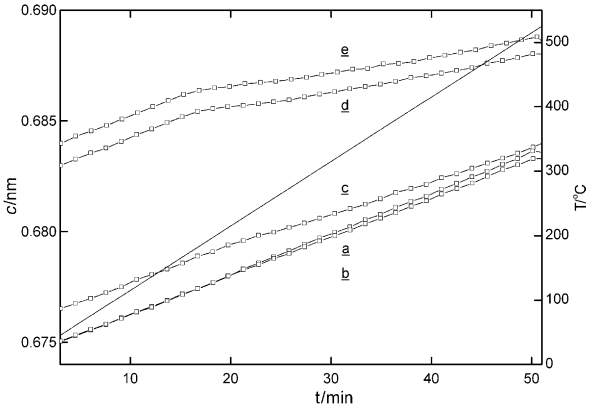

Fig. 6. Graphite c lattice parameter from Rietveld refinement with X-ray diffraction patterns obtained between 25 °C and 525 °C at 10 °C min^{-1}: (□) experimental data, (—) temperature.

consistent with a microscopic thermal expansion coefficient along the c-axis of $\sim 26 \times 10^{-6}$ °C^{-1} – in line with the literature values [13]. (The value of 2.7×10^{-6} °C^{-1} reported by the manufacturer (see Table 1) refers to the transverse macroscopic thermal expansion coefficient of the unirradiated material.) The break in the curves at 180–190 °C, indicating a crystal lattice relaxation, coincides with the inflection point of the rate-of-heat-release peak at 200 °C in the DSC curves. Hence, the Wigner energy release at 200 °C is clearly a result of the lattice relaxation. The effective thermal expansion coefficient of samples d and e above 300 °C is $\sim 12 \times 10^{-6}$ °C^{-1}. Rough linear extrapolation indicates that the c lattice parameter of these samples would reach that of sample a at ~1000 °C.

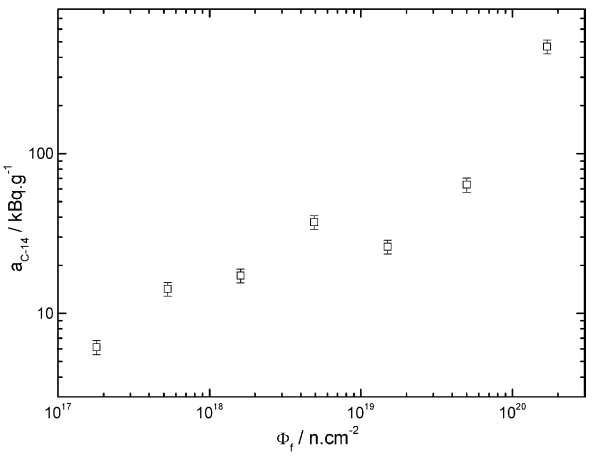

Fig. 7. ^{14}C activity measured by LSC as a function of fast-neutron fluence.

Results of the ^{14}C activity measurements in the inner thermal column graphite are shown in Table 2 and Fig. 7. Each data point is an average of six measurements on each sample aliquot. As expected, the activities are significantly higher than the 1 kBq g^{-1} measured in the outer thermal column and range from 6 kBq g^{-1} for sample a to 467 kBq g^{-1} for sample g. Sample d in the middle of the inner thermal column exhibits an unusually high ^{14}C activity. This would imply a thermal neutron fluence peak in the middle of the inner thermal column – a well-known phenomenon in reactor moderator material [18], as opposed to the fast-neutron fluence peak necessary to explain the anomalous behavior of the sample d as far as Wigner energy is concerned. The thermal neutron fluence entering the inner thermal column (g) has been estimated at 1.1×10^{22} n cm^{-2} [18]. Taking into account only the ^{13}C(n,γ)^{14}C reaction, this would correspond to a ^{14}C activity of ~20 kBq g^{-1}. Consequently, the ^{14}N(n,p)^{14}C reaction must be responsible for the majority of the ^{14}C present in the thermal column. In fact, it has been shown that ^{14}N initially contained as air in the pores of the graphite (see Table 1) would be sufficient to generate about 30 times more ^{14}C, i.e., ~600 kBq g^{-1} [20]. (The inner thermal column has been hermetically sealed in an aluminum liner over the life time of the reactor.) Hence, the total expected ^{14}C activity of ~620 kBq g^{-1} is not significantly different from the value measured in sample g.

The selection and implementation of any treatment and disposal option for irradiated graphite is determined by the Wigner energy content of the material and the potential for self-heating as well as by the inventory of any activation products, ^{14}C and ^{3}H in particular. Even though these two effects are caused by different parts of the neutron spectrum, they are not completely independent and the relationship can get rather complicated. In the case of the ASTRA research reactor graphite, 25% of the blocks from the far end of the outer thermal column exhibited activities below applicable clearance levels, e.g., 80 Bq g^{-1} for ^{14}C. Since Wigner energy accumulation was not a concern either, this material has been cleared and will be reused at another facility. The remaining 75% of the blocks of the outer thermal column could not be cleared because of at least one of the ^{14}C, ^{3}H, ^{60}Co, and ^{152}Eu activities in excess of clearance levels and will be placed in interim storage on site. No thermal treatment is envisioned since, based on the Wigner energy content of the sample a, $\Delta H_{\text{Wigner}} < 25$ J g^{-1}.

The graphite of the inner thermal column exhibits even higher activities and a significant Wigner energy content. Thermal treatment is clearly indicated for at least the first 10 cm of the material. However, since this study had not been completed by the time of the thermal column removal from the reactor, the material from the entire inner thermal column has been treated by heating to 400 °C for 24 h. To contain the potential small ^{14}C releases, the heating of individual graphite blocks has been performed in a furnace placed inside a hot-cell facility. Our results as well as those of Wörner et al. [12] indicate that this is certainly sufficient for eliminating the Wigner energy problem. (Generally, incineration might still be the most reasonable disposal option for irradiated graphite considering the large waste volume reduction factor and the literal disappearance of the Wigner energy issue. However, questions concerning releases of ^{14}C need to be addressed.)

5. Conclusions

The shape of the DSC rate-of-heat-release curves, e.g., maximum at ca. 200 °C and a fine structure at higher temperatures, varies with sample position within the inner thermal column, i.e., the distance from the reactor core. The magnitude of the Wigner energy ranges from 25 to 572 J g^{-1}, the linear Wigner energy accumulation rate is $\sim 7 \times 10^{-17}$ J g^{-1}/n cm^{-2}, and the deviation from linearity begins at a fast-neutron fluence of $\sim 8 \times 10^{17}$ n cm^2. Only the first ~10 cm of graphite closest to the reactor core present a hazard with respect to self-heating and subsequent thermal oxidation. Crystal structure of samples closest to the reactor core (fast-neutron fluence $>1.5-5.0 \times 10^{19}$ n cm^{-2}) is destroyed – a single amorphous peak is present in the XRD patterns at ~12.2° ($c = 0.778$ nm). Crystal structure of samples farther from the reactor core (fast-neutron fluence $<1.5-5.0 \times 10^{19}$ n cm^{-2}) is intact, with marked swelling along the c-axis ($c = 0.675-0.684$ nm, normally 0.672 nm). The dependence of the c lattice parameter on temperature between 25 °C and 200 °C leads to a microscopic thermal expansion coefficient along the c-axis of $\sim 26 \times 10^{-6}$ $°C^{-1}$. However, at 200 °C, coinciding with the maximum in the DSC rate-of-heat-release curves, the rate of thermal expansion abruptly decreases indicating a crystal lattice relaxation. Hence, the Wigner energy release at 200 °C is clearly a result of the lattice relaxation. The ^{14}C activity in the inner thermal column graphite ranges from 6 to 467 kBq g^{-1}. Prior to interim storage or final disposal, thermal treatment of graphite irradiated under similar conditions to a fast-neutron fluence higher than $\sim 5 \times 10^{19}$ n cm^{-2} should be considered. The graphite of the inner thermal column of the ASTRA research reactor has been treated by heating to 400 °C for 24 h in a hot-cell facility prior to interim storage.

Acknowledgements

The first author is indebted to F. Meyer and G. Stolba for bringing the Wigner energy issue to his attention, for providing the graphite material, and for helpful discussions. The samples were machined with great skill by H. Baumgartner. Some of the DSC measurements were performed by M. Dauke as a part of his thesis. The ^{14}C analyses were performed by A. Vesely and H. Lindauer. The contribution of J. Casta in providing the fluence calculations and engaging in many fruitful discussions is gratefully acknowledged.

Funding for the purchase of the The Perkin–Elmer Diamond DSC and DSC 7 instruments has been provided by the Austrian Federal Ministry of Agriculture, Forestry, Environment, and Water Management under Contract No. BMLFUW-Zl. 57 4308/6-V/7/03.

Use of the Advanced Photon Source was supported by the US Department of Energy, Basic Energy Sciences, Office of Energy Research (DOE-BES-OER), under Contract No. W-31-109-Eng-38. The MRCAT beam lines are supported by the member institutions and the US DOE-BES-OER under Contracts DE-FG02-94ER45525 and DE-FG02-96ER45589.

References

[1] E.P. Wigner, CP-387, 1942, p. 4.
[2] T.J. Neubert, M. Burton, R.C. Hirt, A.R. VanDyken, M.G. Bowman, J. Royal, W.R. Burns, A. Novick, R. Maurer, R. Ruder, Neutron-induced discomposition of graphite, Argonne National Laboratory Report ANL-5472, 1956.
[3] In: Proceedings of the Technical Committee Meeting 'Nuclear Graphite Waste Management', IAEA, Manchester, 1999.
[4] F. Meyer, Nucl. Technol. Radiat. Prot. 2 (2003) 61.
[5] D. Lexa, Thermochim. Acta 398 (2003) 241.
[6] A.C. Larson, R.B. Von Dreele, General structure analysis system (GSAS), Los Alamos National Laboratory Report LAUR 86-748, 1994.
[7] F. Seitz, Dicusss. Faraday Soc. 5 (1949) 271.

[8] T. Iwata, J. Nucl. Mater. 133&134 (1985) 361.
[9] S.D. Preston, G.T. Melvin, Rate of release measurements at various heating rates on samples from a Windscale Pile 2 graphite dowel, AEAT, 3169 Issue 2, 1999.
[10] P.C. Minshall, A.J. Wickham, The description of Wigner energy and its release from windscale pile graphite for application to waste packaging and disposal, in [3].
[11] R.M. Guppy, J. McCarthy, S.J. Wisbey, Technical assessment of the significance of Wigner energy for disposal of graphite wastes from the windscale piles, in [3].
[12] J. Wörner, W. Botzem, S.D. Preston, Heat treatment of graphite and resulting tritium emissions, in [3].
[13] B.T. Kelly, B.J. Marsden, K. Hall, D.G. Martin, A. Harper, A. Blanchard, Irradiation damage in graphite due to fast neutrons in fission and fusion systems, IAEA-TECDOC-1154, 2000.
[14] P.A. Thrower, R.M. Mayer, Phys. Status Solidi 47 (1978) 11.
[15] R.H. Telling, C.P. Ewels, A.A. El-Barbary, M.I. Heggie, Nature Mater. 2 (2003) 333.
[16] C.P. Ewels, R.H. Telling, A.A. El-Barbary, M.I. Heggie, P.R. Briddon, Phys. Rev. Lett. 91 (2003) 025505-1–025505-5.
[17] T. Iwata, S. Takamura, H. Maeta, T. Aruga, Displacement cross sections in neutron-irradiated metals, IAEA-TEC-DOC-263, 1982, p. 175.
[18] J. Casta, personal communication, 2005.
[19] G. Erdtmann, Neutron Activation Tables, Verlag Chemie, Weinheim, 1976, p. 23.
[20] A. Vesely, personal communication, 2005.